Rest Profoundly Protects Against Cardiac Remodeling and Benefits Repair

Tami Martino (tmartino@uoguelph.ca)
University of Guelph https://orcid.org/0000-0003-1913-8416
Cristine Reitz
University of Guelph https://orcid.org/0000-0002-1748-0501
Faisal Alibhai
Toronto General Hospital Research Institute, University Health Network
Tarak Khatua
University of Guelph
W. Glen Pyle
University of Guelph

Biological Sciences - Article

Keywords: Evidence-based Experimental Models, Circadian System, Cardiac Remodeling, Slow Functional Decompensation, Heart Disease, Hemodynamic Stress, Myofilament Contractile Function

Posted Date: March 29th, 2021

DOI: https://doi.org/10.21203/rs.3.rs-334421/v1

Version of Record: A version of this preprint was published at JCI Insight on November 22nd, 2022. See the published version at https://doi.org/10.1172/jci.insight.164700.

Abstract

Cardiovascular disease is a leading cause of morbidity and mortality worldwide[1]. Although rest has long been considered beneficial to patients[2], remarkably there are no evidence-based experimental models determining how it benefits disease outcomes. Here, we create a novel experimental rest model in mice, whereby light-induced manipulation of the circadian system briefly extends the rest period by 4 hours each morning. We found, in two different cardiovascular disease conditions (cardiac hypertrophy, myocardial infarction), that imposing a short, extended period of rest each day persistently reduces cardiac remodeling, as compared to control mice subjected to only normal periods of rest, supporting the therapeutic benefits of rest to slow functional decompensation in heart disease. Mechanistically, rest reduces hemodynamic stress on the cardiovascular system, imposing changes on myofilament contractile function in the heart independently consistent within each disease phenotype. Molecular analyses reveal attenuation of cardiac remodeling genes, consistent with the benefits on cardiac structure and function. These same cardiac remodeling genes underlie the pathophysiology of many major human cardiovascular conditions, as demonstrated by interrogating open-source transcriptomic data, and thus patients with other conditions may also benefit from a morning rest period in a similar manner. In summary, we report that rest is a key driver of physiology, leading to the development of an entirely new field on the nature of rest, and provide a strong rationale for advancement of rest based therapy for major clinical diseases.

Main

Cardiovascular disease is a major healthcare and economic burden, with complex clinical phenotypes that frequently progress towards heart failure, for which there is no cure. Circadian rhythms of daily rest and activity contribute to the pathogenesis and pathophysiology of cardiovascular disease[3,4]. Physicians have long aligned with the notion that rest benefits patient outcomes[2]. Indeed Hippocrates, the father of medicine, is quoted as saying “rest as soon as there is pain”. However, clinical recommendations have irrationally tended towards absolute bed rest, resulting in a conundrum as studies infer no benefits or even worse outcomes with complete immobilization in bed[5]. Clinical studies also lack clarity as they focus only on the negative consequences of disruption on the heart, for example due to insufficient sleep[6-9], social jetlag[10], or shiftwork[11]. Similarly, experimental rodent studies also only focus on the adverse effects of circadian disruption or environmental desynchrony on the heart (reviewed in[12-14]), and thus fail to recapitulate the full range of benefits of rest on cardiovascular healing. Indeed, there is little definitive evidence supporting how or why rest benefits heart health and repair. As a result, fundamental physiological and molecular mechanisms of rest remain unclear, and there are no evidence-based data available to benefit individuals with cardiovascular disease. This experimental study in mice co-opts the circadian system to add a short period of early morning rest, in addition to the normal night time rest period, to demonstrate for the first time how rest drives physiologic and molecular responses to benefit cardiovascular disease outcomes.

An ‘extended-rest’ mouse model protects against cardiovascular disease

Rest is a fundamental aspect of human biology, yet little is known about the biological effects of a brief daily rest period on healing of peripheral organs such as the heart. To determine this, male C57BL/6N wild-type mice were subjected to two different heart disease models, each of which recapitulates a major human cardiovascular disease (cardiac hypertrophy, myocardial infarction), followed by imposition of a short extended daily rest period, and benefits were observed *in vivo*. We first examined what happens in pathological cardiac hypertrophy, using the murine transverse aortic constriction (TAC) model. Following recovery from surgery, mice were randomized to either: i) a normal 12 hour (h) light: 12 h dark cycle (normal model; LD 12:12, control) or ii) 12 h light, plus an additional 4 h of blue light (420-520 nm) to stimulate the retinal photoreceptors of the circadian system and delay the onset of activity[15], followed by 8 h dark (rest model; LBD 12:4:8, +Rest). Animals were maintained under these conditions for 4 weeks post-surgery, which recapitulates the cardiac hypertrophy phenotype in this model (Fig. 1a). As expected, the TAC mice developed cardiac hypertrophy, consistent with previous studies[16-18]. In contrast, we found that mice provided additional daily rest post-TAC (TAC+Rest) developed less adverse cardiac remodeling and maintained better cardiac function, as shown by echocardiography (Fig. 1b). Indeed, as compared to TAC hearts from mice maintained on just a normal light: dark cycle, those in the rest group had significantly smaller left ventricular internal dimensions at diastole (LVIDd) and systole (LVIDs) and better ejection fraction (% EF) and fractional shortening (% FS) by 4 weeks *in vivo* (Fig. 1c, Extended Data Table 1). The extended rest period also protected against the development of cardiac hypertrophy (Fig. 1d), as evidenced by significantly smaller heart weight (HW) and HW: body weight (HW:BW) ratios, as compared to controls (Fig. 1e). We next examined what happens in ischemic heart disease, using the permanent left anterior descending coronary artery ligation model of myocardial infarction (MI). Following recovery from surgery, mice were randomized to the same treatment groups, either control (normal LD 12:12), or the rest model (LBD 12:4:8) to stimulate the circadian system mediated delay of activity onset. Animals were maintained for up to 8 weeks post-MI, which recapitulates progression to heart failure in this model (Fig. 1f). As expected, the MI mice developed adverse cardiac remodeling, consistent with our previous studies[19-21]. In contrast, we discovered that the MI+Rest mice developed significantly less left ventricular dilation (Fig. 1g) and longitudinal echocardiographic evaluation revealed better preserved cardiac function by 8 weeks post-MI (Fig. 1h and Extended Data Table 2). The extended rest period also protected against infarct expansion, resulting in smaller scars and better infarct thickness and integrity, as demonstrated by histopathology at 8 weeks post-MI (Fig. 1i-k). Collectively, these data demonstrate using two different models of acquired heart disease, that an additional brief period of rest each morning significantly limits adverse cardiac remodeling and improves long-term outcomes.

Light-induced manipulation of the circadian system to impose rest

The data thus far suggest that exposure to a brief extended daily period of rest profoundly preserves cardiac structure and function in two murine models that mirror the clinical features of human cardiovascular disease. Taking advantage of light as the primary zeitgeber regulating daily circadian rhythms of rest and activity, we evaluated the effects of spectral distribution, as the intrinsically photosensitive melanopsin containing retinal ganglionic cells which mediate most of the effects of light on the circadian mechanism are sensitive to short-wavelength (e.g. blue) but not long-wavelength (e.g. red) light[22-24]. The sensitivity of the circadian system to light for imposing rest in murine heart disease is unknown.

Analysis of 24 h locomotor activity using running wheel actigraphy revealed that an additional 4 h of normal white light during what would otherwise be the start of the active period, resulted in a 4 h extended rest period (Fig. 2a-b). Importantly, with the extended period of rest in the morning hours, the animals still maintained a normal circadian period of ~24 h (Fig. 2a) even though the number of hours per day spent at rest were significantly increased (Fig. 2c). Moreover, we determined that short-wavelength blue light alone (420-520 nm) was sufficient to delay activity onset, while maintaining a normal circadian period of ~24 h (Fig. 2d), thus imposing more hours per day spent at rest (Fig. 2e-f). In contrast, mice exposed to red light showed no change daily activity patterns, as expected, as the circadian system is not sensitive to long-wavelength light (>620 nm) (Extended Data Fig. 1). These observations are consistent with the notion that the rest model mechanistically co-opts the circadian system to interrogate the benefits of a brief daily period of rest on cardiac pathophysiology.

In contrast with our findings in mice subjected to the normal LD 12:12 cycle, we detected reduced hemodynamic load in mice during the extended rest period, by *in vivo* radiotelemetry. Mice had significantly lower systolic (SBP) and diastolic (DBP) blood pressure, concurrent with lower cardiac afterload (mean arterial pressure; MAP) when provided with 4 h of additional rest during the early morning hours (+Rest) (Fig. 2g). Heart rate (HR) was also significantly reduced under the rest model, as compared to controls (Fig. 2h). Our mammalian physiology undergoes profound daily rhythms in blood pressure and heart rate that are important for cardiovascular health[25,26]. A short period of additional rest thus reduces hemodynamic stress on the heart, consistent with the notion that our circadian rhythms critically regulate cardiovascular physiology.

Rest induced contractile function and phosphorylation of sarcomeric myofilaments and precision remodeling in a cardiac disease specific manner

The current paradigm of cardiac pathophysiology holds that the cardiac sarcomere is the basic contractile unit of the heart[27], and that sarcomeric dysfunction drives changes in cardiac muscle contractility central to impaired cardiac function[28]. The structure and function of the cardiac sarcomere is regulated by phosphorylation of the myofilament proteins[28,29]. In heart failure, altered myofilament phosphorylation is a key driver of contractile dysfunction and disease progression[30]. As a result, targeting

the post-translational modification of cardiac myofilaments has become a new frontier in improving cardiac function in heart failure[31]. Our model may provide a novel and promising non-pharmaceutical approach, but the effects of briefly extending morning rest on contractility parameters of the remodeling heart are unknown.

To test for sarcomeric relevance, TAC hearts were first examined using an actomyosin MgATPase activity assay[32]. As compared to healthy hearts under normal L:D conditions, the TAC hearts had significantly reduced maximal MgATPase activity (Fig. 3a), and EC_{50} was similarly decreased (Fig. 3b), suggestive of impaired sarcomere activity at high Ca^{2+} concentrations. These findings coincided with the increased cardiac afterload in the TAC hearts (e.g. MAP) (Fig. 3c). In contrast, with the brief additional period of rest, TAC+Rest hearts had better maximal MgATPase activity (Fig. 3d), normalized EC_{50} (Fig. 3e), and reduced cardiac afterload (Fig. 3f), SBP, DBP and HR (Extended Data Fig. 2a-b), where values were maintained similar to sham controls. Strikingly, and in accordance with our observations at the sarcomere level, TAC+Rest hearts had significantly higher phosphorylation levels of desmin and troponin T (TnT) (Fig. 3g), providing a biological basis underlying reduced stress on the heart. Collectively, these observations are consistent with the notion that the brief morning period of rest offsets pathological myocardial remodeling by preserving contractile function at the level of the cardiac sarcomere.

We next investigated how rest influences sarcomere function in remodeling myocardium post-MI. As compared to healthy hearts under normal L:D, the MI hearts maintained normal actomyosin MgATPase activity at all levels of calcium (Fig. 3h), however we did note that EC_{50} was increased (Fig. 3i), suggestive of a change in myofilament calcium sensitivity, and coinciding with decreased cardiac contractility as demonstrated by reduced dP/dt_{max} and dP/dt_{min} values (Fig. 3j). In contrast, with the brief additional period of rest, MI+Rest hearts had reduced maximal MgATPase activity (Fig. 3k), with no change in EC_{50} (Fig. 3l), suggestive of reduced myofilament energy (ATP) consumption, which coincided with improved cardiac contractility as demonstrated by increased dP/dt_{max} and dP/dt_{min} (Fig. 3m), and by increased SBP and improved left ventricular functional parameters demonstrated by PV loop hemodynamics (Extended Data 2c-g). Moreover, MI+Rest hearts showed improved intrinsic cardiac contractility independent of hemodynamic preload, as evidenced by greater slope of the end-systolic pressure volume relationship (ESPVR) (Extended Data Fig. 2g). Mechanistically, we observed a significant decrease in the phosphorylation of myosin binding protein C (MyBP-C), TnT, and tropomyosin (Tm) in MI+Rest hearts (Fig. 3n), consistent with the reduced myofilament ATPase activity. Thus, rest helps to preserve cardiac contractile function post-MI, which is important for protecting against progression to heart failure. Importantly these data also reveal that rest benefits the heart in a disease phenotype specific manner, remarkable precision medicine tailored to benefit different cardiac pathologies.

Rest responsive pathways in experimental and human cardiovascular disease

Evidence thus far suggests that rest imposes unique structural and functional benefits on the remodeling heart. To elucidate a genetic basis for rest acting on the heart, we used mRNA arrays to quantify the cardiac transcriptomes of healthy mice maintained under the brief daily extended rest period. Beginning with a background set of 28,137 known protein-coding mouse transcripts, principal components analyses clearly identified two different groups of global gene expression, one from the control hearts and one from the extended rest hearts (Fig. 4a). From this, we defined “rest gene” as any gene in the extended rest group identified as robustly expressed on GeneSpring analyses, with at least a >1.3-fold change versus control hearts. In this context we identified 91 rest genes in the heart (Fig. 4b and Supplementary Table 1). Next, we used the Gene Ontology database as a basis for our pathway network, and found many rest genes encode critical regulators of cardiac growth, renewal and remodeling(Fig. 4c and Extended Data Fig. 3). For example, regulator of calcineurin 1 (*Rcan1*)[33], natriuretic peptide B (*Nppb*)[34], REL proto-oncogene, NF-κB subunit (*Rel*)[35], transferrin receptor (*Tfrc*)[36], Egl-9 family hypoxia inducible factor 3 (*Egln3*)[37], ankyrin repeat domain 23 (*Ankrd23*)[38], uncoupling protein 3 (*Ucp3*)[39], pyruvate dehydrogenase kinase 4 (*Pdk4*)[40], actin alpha 1 (*Acta1*)[41], and 3-hydroxy-3-methylglutaryl-CoA synthase 2 (*Hmgsc2*)[42], all of which play critical roles in the pathophysiology of cardiovascular diseases. These biologically significant rest genes were validated by real-time PCR (Fig. 4d).

To test for human relevance, we turned to microarray datasets of control and failing human hearts (Extended Data Table 3). Strikingly, the rest genes and sarcomere gene products identified in our experimental rest studies are clear biomarker targets in human heart disease (Fig. 4e), supporting the notion that rest can benefit both experimental and clinical cardiovascular disease conditions. Seizing upon the recent observation that many clinical drugs target gene products with circadian rhythmicity[43], we also observed that many of our identified rest genes exhibit circadian rhythmicity (Fig. 4f and Extended Data Table 4), and thus can likely be influenced by the molecular clock mechanism consistent with the biological basis of our model system. Finally, to infer whether rest may provide benefits in addition to contemporary drug therapy, we also investigated which of the best-selling and commonly taken heart drugs target rest gene pathways. Notably, 2/3rds of the top prescribed cardiovascular drugs listed by the American Heart Association target rest-responsive gene products pathways (Fig. 4f and Extended Data Table 4), leading us to speculate that drug efficacy can be improved upon in conjunction with an additional brief period of daily rest.

Discussion

The data presented here are consistent with the general hypothesis that rest plays a key role in cardiac remodeling and improves outcomes. Given the limitations of current preclinical models to study rest, we developed a novel murine model that allows us to recapitulate the clinical phenotypes of human heart diseases and study the physiologic and molecular benefits of rest on cardiac repair. We postulate that briefly extending daily rest, by using light to co-opt the circadian biology of rodents, plays a critical role in triggering the pro-cardiac responses. Certainly, the importance of circadian rhythms for cardiovascular health has been demonstrated in experimental[20,44,45] and clinical studies[46,47]. However, while studies

examining the effects of circadian rhythm disruption[16,19] or disturbed sleep[48,49] on cardiovascular healing provide some insights into exacerbating pathophysiology, they do not help explain how to benefit healing, nor provide feasible strategies for patients with cardiovascular disease. Using multiple approaches in preclinical models of heart disease and human gene data from patients with cardiovascular disease, we uncovered evidence implicating rest on benefiting cardiac structure and function, reducing hemodynamic stress, preserving contractile function at the level of the cardiac sarcomere, that rest acts in a precision therapy manner such that it is disease-phenotype specific, and we identified rest genes that have daily rhythms and underlie human heart disease and are common targets of drug therapies (Fig. 4g). Indeed, our findings implicate rest as a master mediator of pathways critical in the pathophysiology of cardiovascular disease.

Strategies to add a brief daily period of rest can be applied alongside and to elevate contemporary therapies for heart disease. Our observations are certainly not conclusive for human patients, but they have enormous implications for benefitting treatment of cardiovascular disease, a leading cause of death worldwide. We hope that our preclinical study will stimulate the initiation of an entirely new field – the nature of rest – along with clinical trials reappraising the value of rest as an important long-term lifestyle approach leading to longer and healthier lives.

Using a remarkably simple strategy, we developed a novel evidence-based murine model to study the benefits of promoting brief daily rest as cardiovascular disease therapy, and especially during the critical early period of cardiovascular pathogenesis and cardiac repair, and which can have applications to healing from any clinical disease.

Declarations

Acknowledgements

This work was supported by grants from the Canadian Institutes of Health Research (CIHR) to T.A.M. C.J.R. is supported by a CIHR PhD award. T.A.M. is a career investigator of the Heart and Stroke Foundation of Canada, and the Distinguished Chair of Molecular Cardiovascular Research at the University of Guelph.

Author contributions

C.J.R. and T.A.M. conceptualized the study and designed the experiments. C.J.R., F.J.A., T.N.K, W.G.P., and T.A.M. performed experiments, analyzed and/or interpreted the experimental results. C.J.R. and T.A.M. prepared the figures and drafted the manuscript. All authors have read and given permission to the paper.

Competing interests

The authors declare no competing interests.

Additional information

Supplementary Information is available for this paper.

Correspondence and requests for materials should be addressed to Dr. Tami A. Martino.

References

1 Roth, G. A. *et al.* Global Burden of Cardiovascular Diseases and Risk Factors, 1990-2019: Update From the GBD 2019 Study. *J Am Coll Cardiol* **76**, 2982-3021, doi:10.1016/j.jacc.2020.11.010 (2020).

2 Babcock, R. H. Rest in the treatment of diseases of the heart. Read at the Meeting of the Tri-State Medical Society at Jacksonville Ill. *JAMA* **XXIII**, 739-741, doi:10.1001/jama.1894.02421250001001 (1894).

3 Martino, T. A. & Sole, M. J. Molecular time: an often overlooked dimension to cardiovascular disease. *Circ Res* **105**, 1047-1061, doi:10.1161/CIRCRESAHA.109.206201 (2009).

4 Martino, T. A. & Young, M. E. Influence of the cardiomyocyte circadian clock on cardiac physiology and pathophysiology. *J Biol Rhythms* **30**, 183-205, doi:10.1177/0748730415575246 (2015).

5 Allen, C., Glasziou, P. & Del Mar, C. Bed rest: a potentially harmful treatment needing more careful evaluation. *Lancet* **354**, 1229-1233, doi:10.1016/s0140-6736(98)10063-6 (1999).

6 Ayas, N. T. *et al.* A prospective study of sleep duration and coronary heart disease in women. *Arch Intern Med* **163**, 205-209 (2003).

7 Alibhai, F. J., Tsimakouridze, E. V., Reitz, C. J., Pyle, W. G. & Martino, T. A. Consequences of Circadian and Sleep Disturbances for the Cardiovascular System. *Can J Cardiol*, doi:10.1016/j.cjca.2015.01.015 (2015).

8 Eckle, T. Editorial: Health Impact and Management of a Disrupted Circadian Rhythm and Sleep in Critical Illnesses. *Curr Pharm Des* **21**, 3428-3430, doi:10.2174/1381612821999150709123504 (2015).

9 Daghlas, I. *et al.* Sleep Duration and Myocardial Infarction. *J Am Coll Cardiol* **74**, 1304-1314, doi:10.1016/j.jacc.2019.07.022 (2019).

10 Wong, P. M., Hasler, B. P., Kamarck, T. W., Muldoon, M. F. & Manuck, S. B. Social Jetlag, Chronotype, and Cardiometabolic Risk. *J Clin Endocrinol Metab* **100**, 4612-4620, doi:10.1210/jc.2015-2923 (2015).

11 Knutsson, A., Akerstedt, T., Jonsson, B. G. & Orth-Gomer, K. Increased risk of ischaemic heart disease in shift workers. *Lancet* **2**, 89-92 (1986).

12 Reitz, C. J. & Martino, T. A. Disruption of Circadian Rhythms and Sleep on Critical Illness and the Impact on Cardiovascular Events. *Curr Pharm Des* **21**, 3505-3511, doi:10.2174/1381612821666150706105926 (2015).

13 Rana, S., Prabhu, S. D. & Young, M. E. Chronobiological Influence Over Cardiovascular Function: The Good, the Bad, and the Ugly. *Circ Res* **126**, 258-279, doi:10.1161/CIRCRESAHA.119.313349 (2020).

14 Thosar, S. S., Butler, M. P. & Shea, S. A. Role of the circadian system in cardiovascular disease. *J Clin Invest* **128**, 2157-2167, doi:10.1172/JCI80590 (2018).

15 Provencio, I. & Foster, R. G. Circadian rhythms in mice can be regulated by photoreceptors with cone-like characteristics. *Brain Res* **694**, 183-190 (1995).

16 Martino, T. A. *et al.* Disturbed diurnal rhythm alters gene expression and exacerbates cardiovascular disease with rescue by resynchronization. *Hypertension* **49**, 1104-1113, doi:10.1161/HYPERTENSIONAHA.106.083568 (2007).

17 Martino, T. A. *et al.* The primary benefits of angiotensin-converting enzyme inhibition on cardiac remodeling occur during sleep time in murine pressure overload hypertrophy. *J Am Coll Cardiol* **57**, 2020-2028, doi:10.1016/j.jacc.2010.11.022 (2011).

18 Tsimakouridze, E. V. *et al.* Chronomics of pressure overload-induced cardiac hypertrophy in mice reveals altered day/night gene expression and biomarkers of heart disease. *Chronobiol Int* **29**, 810-821, doi:10.3109/07420528.2012.691145 (2012).

19 Alibhai, F. J. *et al.* Short-term disruption of diurnal rhythms after murine myocardial infarction adversely affects long-term myocardial structure and function. *Circ Res* **114**, 1713-1722, doi:10.1161/CIRCRESAHA.114.302995 (2014).

20 Bennardo, M. *et al.* Day-night dependence of gene expression and inflammatory responses in the remodeling murine heart post-myocardial infarction. *Am J Physiol Regul Integr Comp Physiol* **311**, R1243-R1254, doi:10.1152/ajpregu.00200.2016 (2016).

21 Reitz, C. J. *et al.* SR9009 administered for one day after myocardial ischemia-reperfusion prevents heart failure in mice by targeting the cardiac inflammasome. *Commun Biol* **2**, 353, doi:10.1038/s42003-019-0595-z (2019).

22 Blume, C., Garbazza, C. & Spitschan, M. Effects of light on human circadian rhythms, sleep and mood. *Somnologie (Berl)* **23**, 147-156, doi:10.1007/s11818-019-00215-x (2019).

23 Berson, D. M., Dunn, F. A. & Takao, M. Phototransduction by retinal ganglion cells that set the circadian clock. *Science* **295**, 1070-1073, doi:10.1126/science.1067262 (2002).

24 Takahashi, J. S., DeCoursey, P. J., Bauman, L. & Menaker, M. Spectral sensitivity of a novel photoreceptive system mediating entrainment of mammalian circadian rhythms. *Nature* **308**, 186-188, doi:10.1038/308186a0 (1984).

25 Clarke, J. M., Hamer, J., Shelton, J. R., Taylor, S. & Venning, G. R. The rhythm of the normal human heart. *Lancet* **1**, 508-512 (1976).

26 Millar-Craig, M. W., Bishop, C. N. & Raftery, E. B. Circadian variation of blood-pressure. *Lancet* **1**, 795-797 (1978).

27 Martin, T. G. & Kirk, J. A. Under construction: The dynamic assembly, maintenance, and degradation of the cardiac sarcomere. *J Mol Cell Cardiol* **148**, 89-102, doi:10.1016/j.yjmcc.2020.08.018 (2020).

28 Hamdani, N. *et al.* Sarcomeric dysfunction in heart failure. *Cardiovasc Res* **77**, 649-658, doi:10.1093/cvr/cvm079 (2008).

29 Lorenzen-Schmidt, I., Clarke, S. B. & Pyle, W. G. The neglected messengers: Control of cardiac myofilaments by protein phosphatases. *J Mol Cell Cardiol* **101**, 81-89, doi:10.1016/j.yjmcc.2016.10.002 (2016).

30 Belin, R. J. *et al.* Augmented protein kinase C-alpha-induced myofilament protein phosphorylation contributes to myofilament dysfunction in experimental congestive heart failure. *Circ Res* **101**, 195-204, doi:10.1161/CIRCRESAHA.107.148288 (2007).

31 Hwang, P. M. & Sykes, B. D. Targeting the sarcomere to correct muscle function. *Nat Rev Drug Discov* **14**, 313-328, doi:10.1038/nrd4554 (2015).

32 Podobed, P. *et al.* The day/night proteome in the murine heart. *Am J Physiol Regul Integr Comp Physiol* **307**, R121-137, doi:10.1152/ajpregu.00011.2014 (2014).

33 Sachan, N. *et al.* Sustained hemodynamic stress disrupts normal circadian rhythms in calcineurin-dependent signaling and protein phosphorylation in the heart. *Circ Res* **108**, 437-445, doi:10.1161/CIRCRESAHA.110.235309 (2011).

34 Goetze, J. P. *et al.* Cardiac natriuretic peptides. *Nat Rev Cardiol* **17**, 698-717, doi:10.1038/s41569-020-0381-0 (2020).

35 Gaspar-Pereira, S. *et al.* The NF-kappaB subunit c-Rel stimulates cardiac hypertrophy and fibrosis. *Am J Pathol* **180**, 929-939, doi:10.1016/j.ajpath.2011.11.007 (2012).

36 Xu, W. *et al.* Lethal Cardiomyopathy in Mice Lacking Transferrin Receptor in the Heart. *Cell Rep* **13**, 533-545, doi:10.1016/j.celrep.2015.09.023 (2015).

37 Xie, L. *et al.* Depletion of PHD3 protects heart from ischemia/reperfusion injury by inhibiting cardiomyocyte apoptosis. *J Mol Cell Cardiol* **80**, 156-165, doi:10.1016/j.yjmcc.2015.01.007 (2015).

38 Buyandelger, B. *et al.* Genetics of mechanosensation in the heart. *J Cardiovasc Transl Res* **4**, 238-244, doi:10.1007/s12265-011-9262-6 (2011).

39 Laskowski, K. R. & Russell, R. R., 3rd. Uncoupling proteins in heart failure. *Curr Heart Fail Rep* **5**, 75-79, doi:10.1007/s11897-008-0013-1 (2008).

40 Cardoso, A. C. *et al.* Mitochondrial Substrate Utilization Regulates Cardiomyocyte Cell Cycle Progression. *Nat Metab* **2**, 167-178 (2020).

41 Lim, D. S., Roberts, R. & Marian, A. J. Expression profiling of cardiac genes in human hypertrophic cardiomyopathy: insight into the pathogenesis of phenotypes. *J Am Coll Cardiol* **38**, 1175-1180, doi:10.1016/s0735-1097(01)01509-1 (2001).

42 Shukla, S. K. *et al.* HMGCS2 is a key ketogenic enzyme potentially involved in type 1 diabetes with high cardiovascular risk. *Sci Rep* **7**, 4590, doi:10.1038/s41598-017-04469-z (2017).

43 Zhang, R., Lahens, N. F., Ballance, H. I., Hughes, M. E. & Hogenesch, J. B. A circadian gene expression atlas in mammals: implications for biology and medicine. *Proc Natl Acad Sci U S A* **111**, 16219-16224, doi:10.1073/pnas.1408886111 (2014).

44 Young, M. E., Razeghi, P., Cedars, A. M., Guthrie, P. H. & Taegtmeyer, H. Intrinsic Diurnal Variations in Cardiac Metabolism and Contractile Function. *Circulation Research* **89**, 1199-1208, doi:10.1161/hh2401.100741 (2001).

45 Martino, T. A. *et al.* Circadian rhythm disorganization produces profound cardiovascular and renal disease in hamsters. *Am J Physiol Regul Integr Comp Physiol* **294**, R1675-1683, doi:10.1152/ajpregu.00829.2007 (2008).

46 Muller, J. E., Tofler, G. H. & Stone, P. H. Circadian variation and triggers of onset of acute cardiovascular disease. *Circulation* **79**, 733-743, doi:10.1161/01.cir.79.4.733 (1989).

47 Scheer, F. A. *et al.* Impact of the human circadian system, exercise, and their interaction on cardiovascular function. *Proc Natl Acad Sci U S A* **107**, 20541-20546, doi:10.1073/pnas.1006749107 (2010).

48 Krittanawong, C. *et al.* Association between short and long sleep durations and cardiovascular outcomes: a systematic review and meta-analysis. *Eur Heart J Acute Cardiovasc Care*, 2048872617741733, doi:10.1177/2048872617741733 (2017).

49 Javaheri, S. *et al.* Sleep apnea in 81 ambulatory male patients with stable heart failure. Types and their prevalences, consequences, and presentations. *Circulation* **97**, 2154-2159, doi:10.1161/01.cir.97.21.2154 (1998).

Methods

Experimental animals

All studies were carried out in accordance with the guidelines of the Canadian Council on Animal Care and were reviewed and approved by the University of Guelph Institutional Animal Care and Use Committee. All animals were housed at the University of Guelph Central Animal Facilities. Standard rodent chow and water were provided *ad libitum*. Rest and activity were recorded from 8-week-old male C57BL/6N mice (Charles River Laboratories), using individual cages equipped with running wheels (Colbourn Instruments), as described[21,50], and data were collected and analyzed using ClockLab Software (Actimetrics). Rest was measured as hours per day with < 100 counts of activity. Animals were placed on either i) a “control” normal light (L) dark (D) cycle (LD 12:12), or ii) an extended light cycle to induce rest using white light (LD 16:8), or iii) an extended period of light under red light (>620 nm wavelength; LR 12:12) or iv) “extended rest” induced by blue light (420-520 nm wavelength, LBD 12:4:8, rest model) targeting the circadian system to manipulate rest and activity. Light wavelengths were filtered using blue Roscolux 74 or red Roscolux 27 (Rosco Laboratories) over white fluorescent lights (Octron T8; Sylvania). Cardiac hypertrophy was surgically induced by transverse aortic constriction (TAC) as previously described[16-18,50]. Myocardial infarction was surgically induced by left anterior descending coronary artery ligation as described[19,51]. All surgeries were performed between zeitgeber time (ZT) 01 and ZT04 to avoid confounding circadian effects, and used the same methods for anesthesia, intubation, and analgesia as previously described, and mice were given a subcutaneous injection of buprenorphine (0.1 mg/kg) for post-operative analgesia upon awakening, and at 8 hours and 24 hours post-operatively. Following recovery, starting on the first night post-surgery, mice were housed under control or extended light regimens for up to 8 weeks.

Echocardiography

Cardiac structure and function were assessed at baseline, 1- and 4-weeks post-TAC, or at baseline, 1-, 4-, and 8-weeks post-MI using a GE Vivid e90 ultrasound machine (GE Medical Systems) with an L8-18i-D 15 MHz linear array transducer under light anesthesia (1.0% isoflurane). Images were analyzed on an offline system using EchoPAC (GE Medical Systems). Measurements were taken at the mid-papillary level and used to determine left ventricular internal dimension at diastole (LVIDd), left ventricular internal dimension at systole (LVIDs), % ejection fraction (% EF), % fractional shortening (% FS), interventricular septal wall thickness at diastole (IVSd), left ventricular posterior wall thickness at diastole (LVPWd), and heart rate (HR). For the TAC studies, a total of 44 mice were used (n = 11 mice/group). For the MI studies, 20 mice were used (n = 10 mice/group). At least 5 images per animal were used for analysis, and means are presented.

In vivo pressure-volume hemodynamics

At 8 weeks post-MI, mice were anesthetized with 4% isoflurane, intubated, and ventilated. A 1.2Fr pressure-volume catheter (Transonic) was inserted via the right carotid artery and advanced into the ascending aorta for blood pressure measurements. The catheter was then advanced into the LV. Real time physiologic LV and aortic pressure measurements were recorded on an ADInstrument PowerLab, including left ventricular end systolic pressure (LVESP), diastolic pressure (LVEDP), systolic volume (LVESV), diastolic volume (LVEDV), stroke volume (SV), cardiac output (CO), maximum and minimum first derivatives of LV pressure (dP/dt_{max}; dP/dt_{min}), and systolic/diastolic blood pressures (SBP/DBP). Mean arterial blood pressure (MAP) was calculated as DBP + (SBP-DBP)/3. After PV measurements were obtained, the inferior vena cava was briefly occluded to block venous return to determine the end-systolic PV relationship[52]. Continuously recorded pressures were analyzed with Lab Chart 7 (Colorado Creeks, USA). A total of 18 mice were used (n = 9 mice/group), with data reported as mean ± s.e.m.

In vivo radiotelemetry

Diurnal cardiovascular hemodynamics was assessed using PA-C10 murine telemetry probes (Data Sciences International) to collect continuous blood pressure and heart rate data from conscious, freely moving mice, as previously described[17,50]. Animals were anesthetized with 4% isoflurane, intubated, ventilated (model 687; Harvard Apparatus), and maintained at 2.5% isoflurane throughout the procedure. The right carotid artery was isolated and the telemeter catheter was implanted to the level of the aortic arch via the carotid artery. The telemeter transmitter unit was implanted in a subcutaneous skin pouch and the neck incision was closed using silk 6-0 suture (Covidien). Mice were administered buprenorphine (0.1 mg per kg) analgesia upon awakening and at 8 hours and 24 hours postoperatively. Recordings were initiated at 1 week following telemeter implantation and measurements were collected over three continuous 24-hour cycles for each light condition. Following baseline telemetry recordings, mice were subjected to transverse aortic constriction (TAC) surgery. At 4 weeks post-TAC, measurements were collected over three additional days under each light cycle. Systolic (SBP) and diastolic (DBP) blood pressure, mean arterial pressure (MAP), and heart rate (HR) were analysed using the Data Quest IV system (Data Sciences International). Measurements were taken every 5 min for 30 seconds and averaged into 1-hour bins according to ZT time. A total of 4 mice were used, enabling a paired analysis of the same mice before and after all experimental interventions, with data reported as mean ± s.e.m.

Histology

At 8 weeks post-MI, mice were euthanized following hemodynamic assessments with isoflurane and cervical dislocation. Body weight (BW), heart weight (HW) and tibia length (TL) were measured for each animal. Hearts were removed, perfused with 1 M KCl, fixed in 10% neutral buffered formalin for 48 h, and

paraffin embedded. Hearts were then sectioned at 5 μm thickness, from apex to base, collecting 10 sections every 300 μm. Sections were stained with Masson's trichrome, mounted using Cytoseal 60 mounting media (Thermo Scientific) and visualized with a Nikon E600 microscope using Q-Capture software (QImaging; Surrey, BC) and quantified using Image J 1.46 (NIH). Infarct thickness was determined from a minimum of 5 measurements/section over equidistant points along the infarct region. LV diameter was determined from sections collected at mid-papillary level. Relative infarct size was determined by dividing the sum of the endocardial and epicardial circumference occupied by the infarct by the sum of the total LV epicardial and endocardial circumferences. A total of 10 mice were used (n = 5 mice/group), with data presented as mean ± s.e.m.

Myofilament isolation, actomyosin MgATPase assay, and protein phosphorylation

At 4 weeks post-surgery. TAC, MI and sham animals were euthanized by isoflurane and cervical dislocation at ZT15. Hearts were collected, snap frozen in liquid nitrogen, and stored at -80°C until use. Cardiac myofilaments were isolated by differential centrifugation using the protocol described by Podobed *et al.*[32]. Actomyosin MgATPase activity in isolated cardiac myofilaments was determined using a modified Carter assay, as described previously[19,32]. Isolated myofilament proteins were separated using 12% sodium dodecyl sulfate-polyacrylamide gel electrophoresis and protein phosphorylation levels were quantified using the PRO-Q Diamond phosphoprotein gel stain (Invitrogen), following the protocol of Podobed *et al.*[32]. Gels were then stained with Coomassie to determine total protein. Gel imaging was performed on a Bio-Rad ChemiDoc MP Imaging System (Bio-Rad) and analysed using ImageJ (NIH) with protein phosphorylation normalized to total protein. Samples were run, stained, and imaged at the same time on separate gels, and normalized to actin.

RNA isolation, microarray, and bioinformatics analyses

After 4 weeks under either the rest model or control conditions, healthy mice were euthanized by isoflurane and cervical dislocation at ZT07. Hearts were collected and snap frozen in liquid nitrogen and stored at -80°C until use. Total RNA from murine heart tissue was isolated using the miRNeasy Mini Kit (Qiagen), as previously described[50]. RNA quantity and quality were assessed by Nanodrop (260/280 ≥ 2; Thermo Scientific) and RNA ScreenTape (RIN ≥ 7; Agilent). Whole genome microarray analyses were performed using the Affymetrix GeneChip Mouse Gene 2.0 ST array, which interrogates 35,240 RefSeq coding and non-coding transcripts (GEO Accession: GSE115567). Gene expression analyses were performed on 6 individual mouse heart samples. Bioinformatics analyses were performed using GeneSpring GX v14.9 (Agilent Technologies). Raw .cel files were loaded into a project file with exon analysis and Affymetrix exon expression experiment settings and a biological significance workflow analysis. The most recent mouse gene 2.0 ST array annotation technology (MoGene-2_0-st_na36_mm10_2016-07-06) was used to perform all analyses. Raw fluorescence data were normalized

across all chips using the exon robust multiarray summarization algorithm. Experiment parameters for sample groups and replicate structure were defined, and launched as a group-level interpretation. Quality control across all samples was assessed by log2(normalized signal values) expression of 8 control hybridization probes across all chips, and group level clustering was analyzed by principal components analysis. The probeset filter parameter was defined to include all 34,351 probeset entities, then filtered by expression using a lower cut-off of 60 raw fluorescence units. Differentially expressed genes were determined by fold change analysis of all entities with ≥ 1.3-fold change in expression between rest vs. control hearts (Supplementary Table 1). Hierarchical cluster analysis of this gene cassette generated heat maps of entity expression relative to control hearts. Gene Ontology (GO) analysis was performed on differentially expressed gene lists using the Database for Annotation, Visualization, and Integrated Discovery (DAVID) Functional Annotation Tool (DAVID Bioinformatics 6.8, NIAID/NIH)[53]. Circos plots were generated using Circos v.0.69-9[54].

Quantitative real time polymerase chain reaction (qRT-PCR)

Analysis of mRNA expression by qRT-PCR was performed on a ViiA7 real time PCR system (Applied Biosystems) using the Power SYBR Green RNA-to-Ct one step kit (Life Technologies) under the following protocol: reverse transcription at 48°C for 30 min and 95°C for 10 min for 1 cycle, followed by amplification at 95°C for 15 sec and 60°C for 1 min for 40 cycles, followed by hold at room temperature. The following RT-PCR primer sequences were used, including forward and reverse sequences for each gene, respectively:

Rcan1 exon 4 isoform mouse CCCGTGAAAAAGCAGAATGC, TCCTTGTCATATGTTCTGAAGAGGG; *Nppb* mouse GCGAGACAAGGGAGAACAC, GCGGTGACAGATAAAGGAAAAG; *Rel* mouse CAGAGTGACTTCAAGGGAAC, GTTAGGCACCGAGTCTTTAG; *Tfrc* mouse CACTCGCCCAAGTTATATCC, GCACGGTGATACTCATACTG; *Egln3* mouse CCCGAACTCTGTACGAAAC, CTGCTTGTGGGATTCTAGC; *Ankrd23* mouse TCCAGGGCATGAGAGAAG, GGCTGCTACTGGTAGAAATG; *Ucp3* mouse CCCAACATCACAAGAAATGCC, ACAGAAGCCAGCTCCAAAG; *Pdk4* mouse CGCCAGAATTAAACCTCACAC, TTCTTGATGCTCGACCGTG; *Acta1* mouse AGACCTTCAACGTGCCTG, CGTCCCCAGAATCCAACAC; *Hmgcs2* mouse CACCTGCTACTAACCTTG, CAAGAGGACACTTTCAGG; histone mouse GCAAGAGTGCGCCCTCTACTG, GGCCTCACTTGCCTCCTGCAA. Relative gene expression was normalized to histone using the delta delta CT method, as described previously[19,20].

Human myocardial gene expression microarray analyses

Human myocardial gene expression data were obtained using publicly available datasets from the Gene Expression Omnibus (GEO) database[55]. Raw .cel microarray files were downloaded from 6 independent datasets examining myocardial gene expression from LV biopsies from a total of 140

patients. Datasets included patients with aortic stenosis (AS)[56], dilated cardiomyopathy (DCM)[57-59], ischemic cardiomyopathy (ICM)[58-60], and non-failing controls (GEO datasets: GSE1145 (AS), GSE10161 (AS), GSE3585 (DCM), GSE42955 (DCM, ICM), GSE79962 (DCM, ICM), GSE16499 (ICM); see Extended Data Table 3). Raw microarray files were analysed from each dataset, using GeneSpring GX v14.9 (Agilent Technologies Inc.), as described above. All probeset entity lists were then interrogated for rest-responsive genes identified from our murine studies, and analysed as fold change in expression from non-failing control hearts. See Extended Data Table 3 for *n*-values and microarray technologies for each dataset.

Cardiac medications targeting rest pathways

A list of the top 66 commonly prescribed cardiovascular medications was obtained from the American Heart Association (AHA) website[61]. All molecular drug targets were determined using the DrugBank database[62]. Lists were then curated for target genes with known rhythmic transcripts (JTK *P*-value < 0.05) based on analyses from mouse heart tissue using the CircaDB database[63] and for rest-responsive genes identified from our rest model microarray analyses in the murine heart.

Statistical analyses

Values are presented as mean ± s.e.m. Statistical comparisons were made by paired or unpaired Student's *t*-test, as applicable. All analyses were performed using GraphPad Prism 8 (GraphPad Software) or Excel (Microsoft). A *P*-value ≤ 0.05 was considered statistically significant. All endpoints, *n*-values, and statistics are provided in detail in the Figure legends and in the Extended Data.

Data availability

The authors declare that all supporting data are available with the article, extended data, supplementary files, or from the corresponding author upon reasonable request. Microarray data were deposited to the GEO database, accession #GSE115567.

Publicly available microarray datasets were downloaded and analyzed from the GEO database, as described in the methods and outlined in Extended Data Table 3.

Methods References

16 Martino, T. A. *et al.* Disturbed diurnal rhythm alters gene expression and exacerbates cardiovascular disease with rescue by resynchronization. *Hypertension* **49**, 1104-1113, doi:10.1161/HYPERTENSIONAHA.106.083568 (2007).

17 Martino, T. A. *et al.* The primary benefits of angiotensin-converting enzyme inhibition on cardiac remodeling occur during sleep time in murine pressure overload hypertrophy. *J Am Coll Cardiol* **57**, 2020-2028, doi:10.1016/j.jacc.2010.11.022 (2011).

18 Tsimakouridze, E. V. *et al.* Chronomics of pressure overload-induced cardiac hypertrophy in mice reveals altered day/night gene expression and biomarkers of heart disease. *Chronobiol Int* **29**, 810-821, doi:10.3109/07420528.2012.691145 (2012).

19 Alibhai, F. J. *et al.* Short-term disruption of diurnal rhythms after murine myocardial infarction adversely affects long-term myocardial structure and function. *Circ Res* **114**, 1713-1722, doi:10.1161/CIRCRESAHA.114.302995 (2014).

20 Bennardo, M. *et al.* Day-night dependence of gene expression and inflammatory responses in the remodeling murine heart post-myocardial infarction. *Am J Physiol Regul Integr Comp Physiol* **311**, R1243-R1254, doi:10.1152/ajpregu.00200.2016 (2016).

21 Reitz, C. J. *et al.* SR9009 administered for one day after myocardial ischemia-reperfusion prevents heart failure in mice by targeting the cardiac inflammasome. *Commun Biol* **2**, 353, doi:10.1038/s42003-019-0595-z (2019).

32 Podobed, P. *et al.* The day/night proteome in the murine heart. *Am J Physiol Regul Integr Comp Physiol* **307**, R121-137, doi:10.1152/ajpregu.00011.2014 (2014).

50 Alibhai, F. J. *et al.* Disrupting the key circadian regulator CLOCK leads to age-dependent cardiovascular disease. *J Mol Cell Cardiol* **105**, 24-37, doi:10.1016/j.yjmcc.2017.01.008 (2017).

51 Mistry, P. *et al.* Circadian influence on the microbiome improves heart failure outcomes. *J Mol Cell Cardiol* **149**, 54-72, doi:10.1016/j.yjmcc.2020.09.006 (2020).

52 Wang, W. *et al.* Loss of Apelin exacerbates myocardial infarction adverse remodeling and ischemia-reperfusion injury: therapeutic potential of synthetic Apelin analogues. *Journal of the American Heart Association* **2**, e000249, doi:10.1161/JAHA.113.000249 (2013).

53 Huang da, W., Sherman, B. T. & Lempicki, R. A. Systematic and integrative analysis of large gene lists using DAVID bioinformatics resources. *Nat Protoc* **4**, 44-57, doi:10.1038/nprot.2008.211 (2009).

54 Krzywinski, M. *et al.* Circos: an information aesthetic for comparative genomics. *Genome Res* **19**, 1639-1645, doi:10.1101/gr.092759.109 (2009).

55 Edgar, R., Domrachev, M. & Lash, A. E. Gene Expression Omnibus: NCBI gene expression and hybridization array data repository. *Nucleic Acids Res* **30**, 207-210, doi:10.1093/nar/30.1.207 (2002).

56 Petretto, E. *et al.* Integrated genomic approaches implicate osteoglycin (Ogn) in the regulation of left ventricular mass. *Nat Genet* **40**, 546-552, doi:10.1038/ng.134 (2008).

57 Barth, A. S. *et al.* Identification of a common gene expression signature in dilated cardiomyopathy across independent microarray studies. *J Am Coll Cardiol* **48**, 1610-1617, doi:10.1016/j.jacc.2006.07.026 (2006).

58 Molina-Navarro, M. M. *et al.* Differential gene expression of cardiac ion channels in human dilated cardiomyopathy. *PLoS One* **8**, e79792, doi:10.1371/journal.pone.0079792 (2013).

59 Matkovich, S. J. *et al.* Widespread Down-Regulation of Cardiac Mitochondrial and Sarcomeric Genes in Patients With Sepsis. *Crit Care Med* **45**, 407-414, doi:10.1097/CCM.0000000000002207 (2017).

60 Kong, S. W. *et al.* Heart failure-associated changes in RNA splicing of sarcomere genes. *Circ Cardiovasc Genet* **3**, 138-146, doi:10.1161/CIRCGENETICS.109.904698 (2010).

61 AHA. American Heart Association. Cardiac Medications. 2019. Available at: https://www.heart.org/en/health-topics/heart-attack/treatment-of-a-heart-attack/cardiac-medications. Accessed August 20, 2019. (2019).

62 Wishart, D. S. *et al.* DrugBank 5.0: a major update to the DrugBank database for 2018. *Nucleic Acids Res* **46**, D1074-D1082, doi:10.1093/nar/gkx1037 (2018).

63 Pizarro, A., Hayer, K., Lahens, N. F. & Hogenesch, J. B. CircaDB: a database of mammalian circadian gene expression profiles. *Nucleic Acids Res* **41**, D1009-1013, doi:10.1093/nar/gks1161 (2013).

Figures

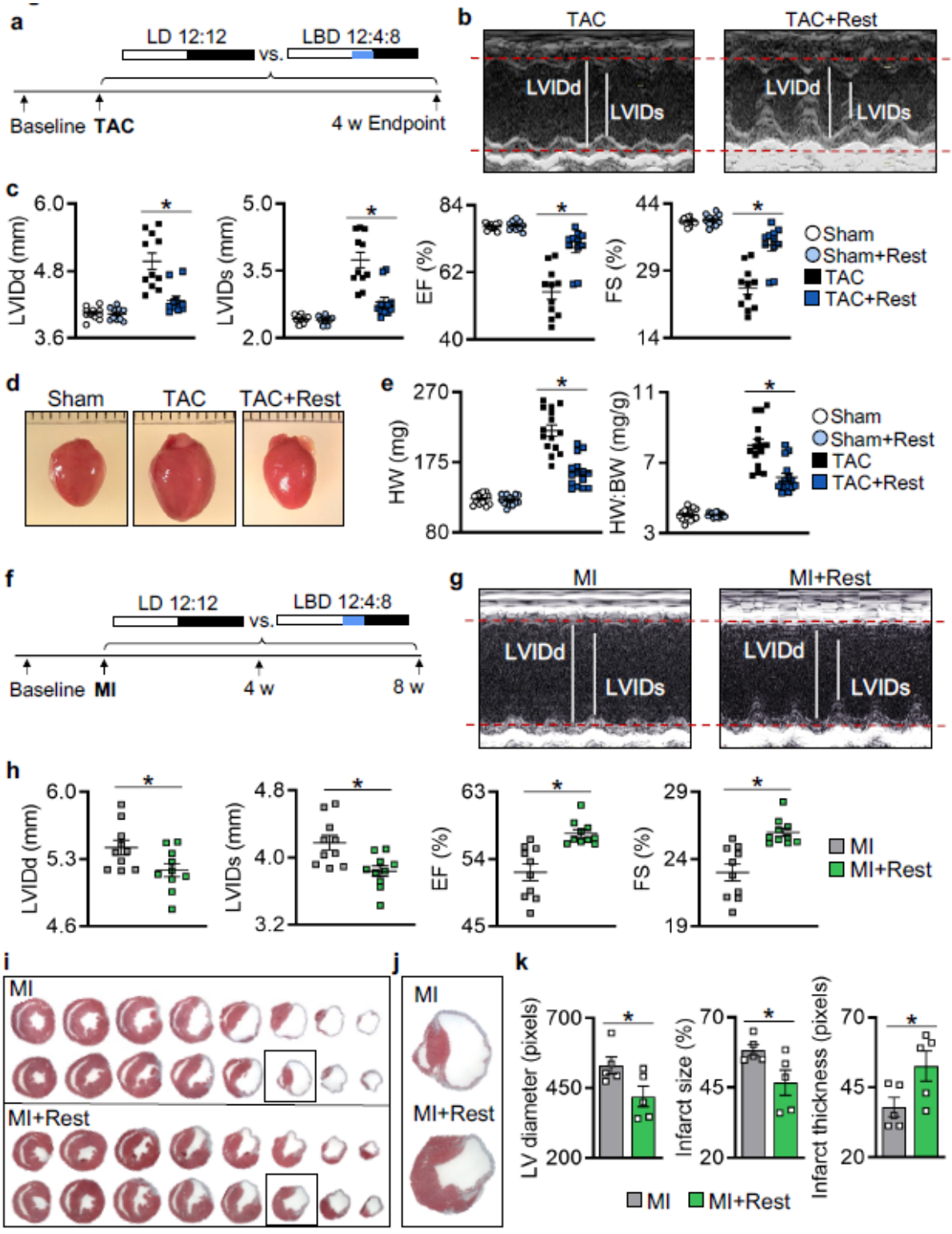

Figure 1

Rest benefits outcomes in both hypertrophic and ischemic heart disease. a, Rest model and cardiac hypertrophy experimental design, mice underwent baseline echocardiography followed by transverse aortic constriction (TAC) and were randomized to control conditions (12 hours (h) light: 12 h dark; LD 12:12) vs. the rest model (12 h light: 4 h blue light: 8 h dark; LBD 12:4:8) for up to 4 weeks. b, Representative M-mode echocardiography images at 4 weeks post-TAC, showing (c) smaller left

ventricular internal dimensions at diastole (LVIDd) and systole (LVIDs) and better % ejection fraction (EF) and fractional shortening (FS) in mice housed under the rest model. n=11 mice/group. d, Representative images and (e) quantification of heart weight (HW) and HW: body weight (BW) at 4 weeks post-TAC. n=15 mice/group. *P<0.001 TAC vs. TAC+Rest, by unpaired Student's t-test. f, Rest model and myocardial infarction (MI) experimental design. g, Representative M-mode echocardiography at 8 weeks post-MI, showing (h) smaller LVIDd and LVIDs and better % EF and % FS in mice under the rest model. n=10 mice/group. i, Representative histopathology, (j) close-up of infarct region, and (k) quantification of LV diameter and infarction expansion and integrity in MI+Rest hearts at 8 weeks post-MI. n=5 mice/group. *P<0.05 MI vs. MI+Rest, by unpaired Student's t-test. Data are represented as mean ± s.e.m.

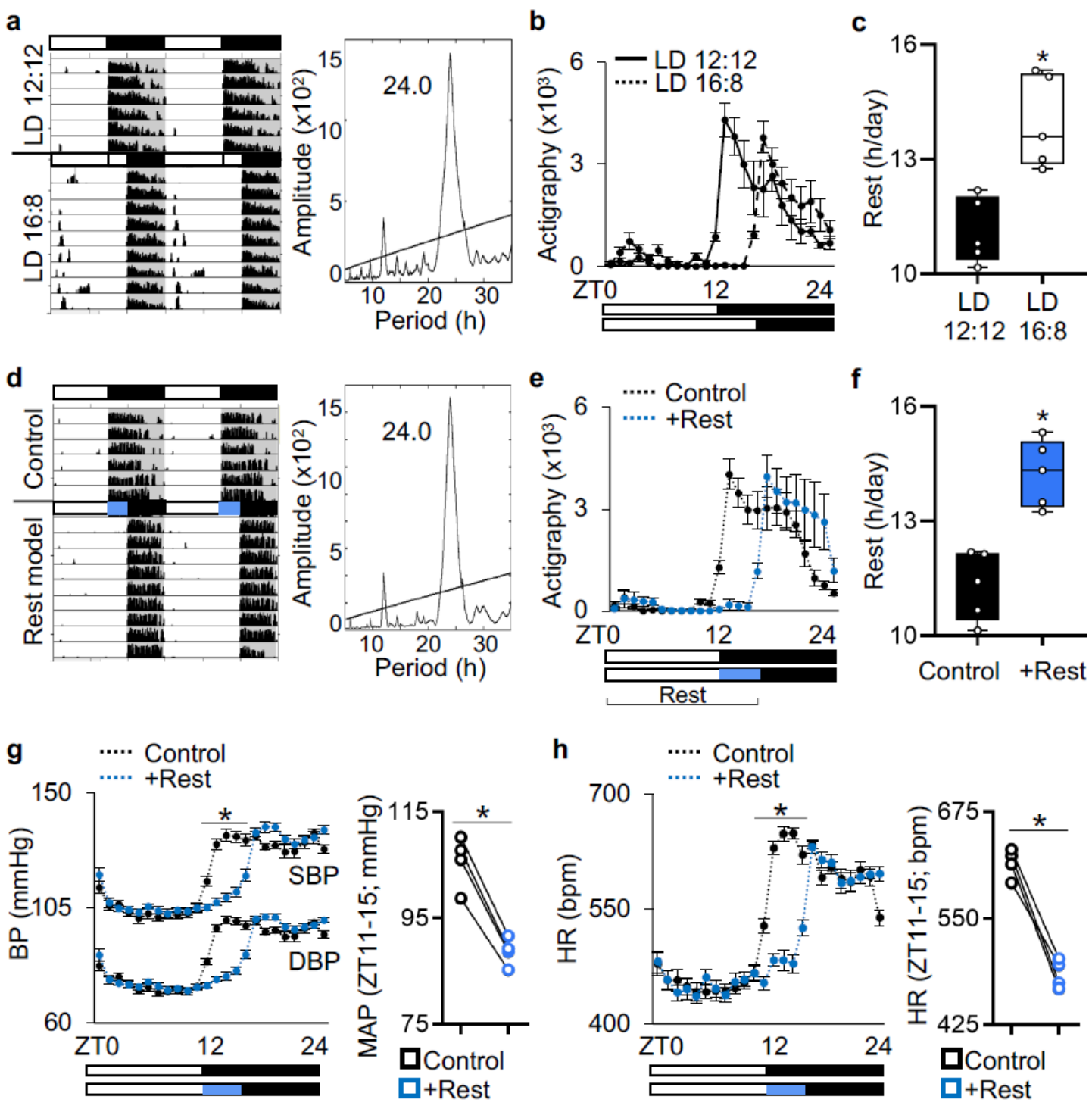

Figure 2

Diurnal rest-activity rhythms and cardiovascular hemodynamics in a mouse model of rest. a, Representative actigraphy and periodogram, (b) activity quantification, and (c) hours of rest per day in mice under normal 12 h light: 12 h dark (LD 12:12) vs. extended light (LD 16:8). n=5 mice/group. d, Representative actigraphy and periodogram, (e) activity quantification, and (f) hours of rest per day in mice under the rest model (+Rest) vs. control. n=5 mice/group. g, Diurnal rhythms in systolic (SBP) and diastolic (DBP) blood pressure and quantification of average mean arterial pressure (MAP) from zeitgeber time (ZT) 11-15, and (h) diurnal heart rate (HR) in healthy mice under rest model vs. control. n=4 mice/group. *P<0.001 Control vs. +Rest, paired Student's t-test. Data are represented as mean ± s.e.m.

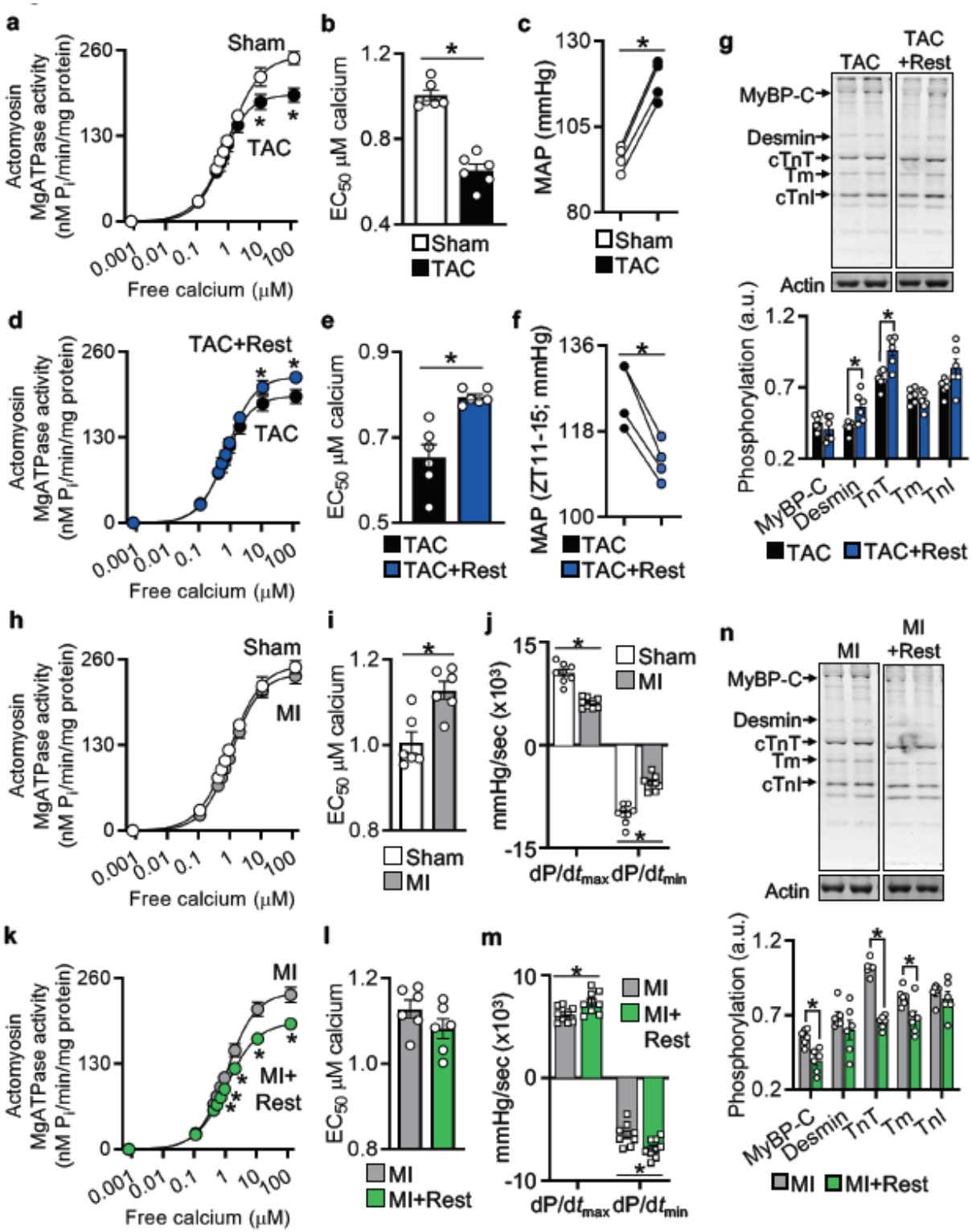

Figure 3

Rest reduces cardiac workload through intrinsic effects on the cardiac myofilaments. a, Cardiac actomyosin MgATPase activity and (b) EC50 are reduced at 4 weeks post-TAC, (c) consistent with pathological cardiac afterload (mean arterial pressure; MAP) in the TAC model. d, Myofilament activity, (e) EC50, and (f) MAP are normalized in TAC+Rest hearts, (g) consistent with increased myofilament protein phosphorylation. h, Cardiac actomyosin MgATPase activity is maintained at 4 weeks post-MI, (i) with

increased EC50, (j) concurrent with reduced in vivo cardiac contractility in the MI model. k, Extended rest lowers myofilament ATP consumption, (l) but not EC50, (m) consistent with better in vivo cardiac contractility, and (n) reduced myofilament protein phosphorylation. Murine heart tissue collected at ZT15, 4 weeks post-surgery. n=6/group for ATPase and phosphorylation, n=4/group for in vivo radiotelemetry, n=9/group for in vivo pressure-volume hemodynamics. For MgATPase data *P<0.005, for all other data *P<0.05, by unpaired Student's t-test. Data are represented as mean ± s.e.m.

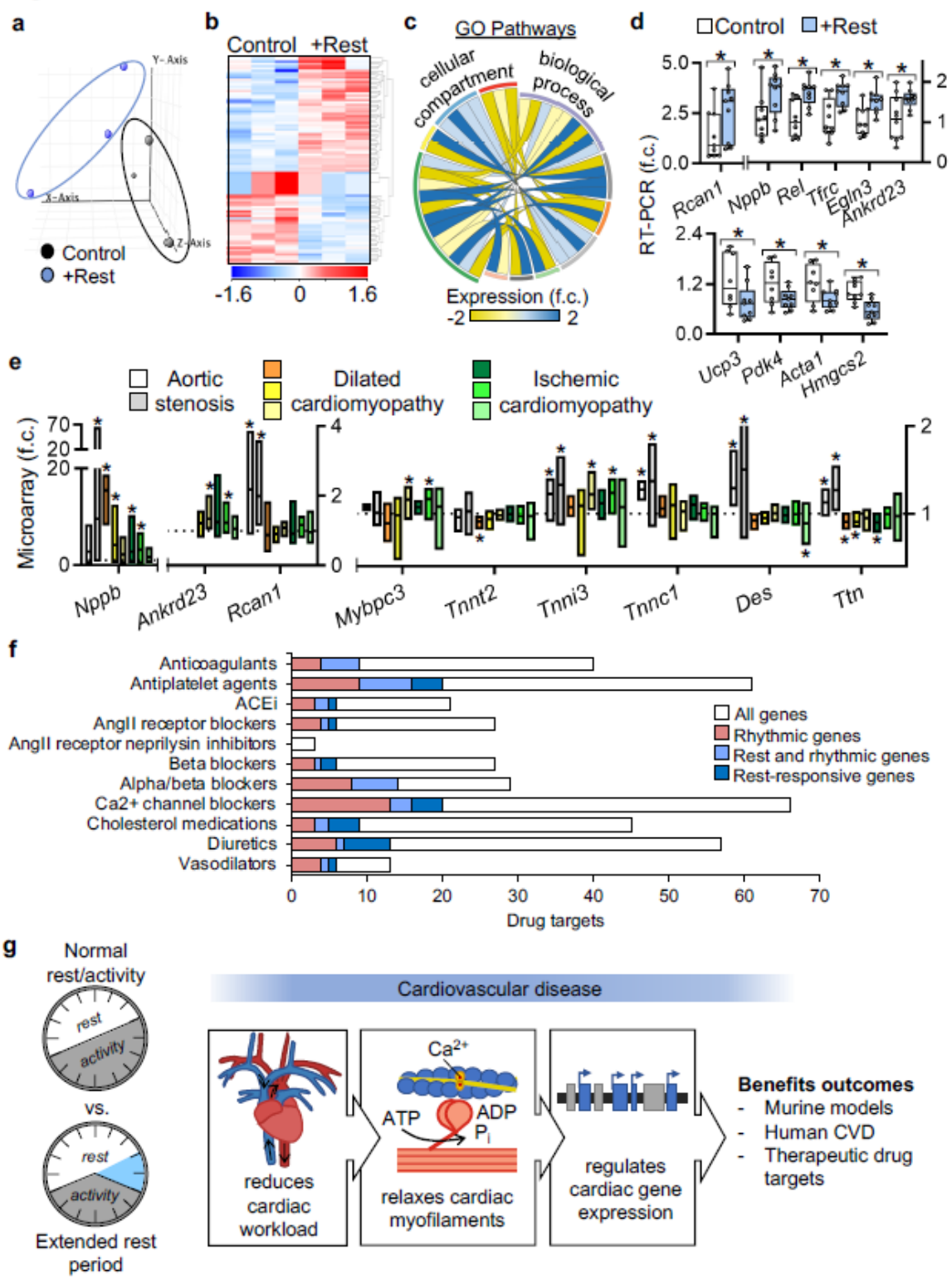

Figure 4

Rest regulates cardiac gene expression with implications for human heart disease. a, Principal components analysis of cardiac transcriptome from healthy controls or mice maintained under the rest model (+Rest) for 4 weeks. Hearts were collected during the middle of the rest period (ZT07). b, Differentially regulated genes (fold change ≥ 1.3) in control vs. rest model. c, Gene ontology (GO) cellular compartment and biological process correlations, up-regulated (blue) or down-regulated (yellow) with rest. See Extended Data Fig. 3. d, RT-PCR of cardiac biomarkers up- and down-regulated in the heart with rest, pooled across the rest period (ZT03, 07, 11). n=9/group from n=3/timepoint, *P<0.05 Control vs. +Rest, unpaired Student's t-test. e, Open-source human heart tissue gene bioinformatics of cardiac remodeling and myofilament genes. *P<0.05 vs. non-failing controls, unpaired Student's t-test. f, Rhythmic and rest-responsive genes encode molecular drug targets (including enzymes, transporters, and carriers) of commonly prescribed cardiac medications. (g) A novel mouse model of extended rest reveals how rest reduces cardiac hemodynamic workload, relaxes the cardiac myofilaments, and regulates cardiac gene profiles to benefit outcomes in cardiovascular disease. Data are represented as mean ± s.e.m.

Supplementary Files

This is a list of supplementary files associated with this preprint. Click to download.

- Reitzetal.RestandtheHeartSupplementaryInformationMar16.docx
- ReitzetalExtendedDataFig1.pdf
- ReitzetalExtendedDataFigure2.pdf
- ReitzetalExtendedDataFigure3.pdf
- ReitzetalExtendedDataTable1.pdf
- ReitzetalExtendedDataTable2.pdf
- ReitzetalExtendedDataTable3.pdf
- ReitzetalExtendedDataTable4.pdf